Article

A-Kinase Anchoring Proteins Diminish TGF-β1/ Cigarette Smoke-Induced Epithelial-to-Mesenchymal Transition

Haoxiao Zuo[1-3], Irene H. Heijink[2,4,5], Christina H.T.J. van der Veen[1], Laura Hesse[2,4], Klaas Nico Faber[6], Wilfred J. Poppinga[1,2], Harm Maarsingh[7], Viacheslav O. Nikolaev[3,8] and Martina Schmidt[1,2]*

[1] University of Groningen, Department of Molecular Pharmacology, Groningen, The Netherlands; ; haoxiaozuo1212@gmail.com (H.Z.), c.h.t.j.van.der.veen@rug.nl (C.H.T.J.v.d.Veen), wilfredpoppinga@gmail.com (W.J.P.), m.schmidt@rug.nl (M.S.)

[2] University of Groningen, University Medical Center Groningen, Groningen Research Institute for Asthma and COPD, GRIAC, Groningen, The Netherlands; haoxiaozuo1212@gmail.com (H.Z.), l.hesse@umcg.nl (L.H.), m.schmidt@rug.nl (M.S.)

[3] Institute of Experimental Cardiovascular Research, University Medical Centre Hamburg-Eppendorf, 20246 Hamburg, Germany; haoxiaozuo1212@gmail.com (H.Z.), v.nikolaev@uke.de (V.O.N.)

[4] University of Groningen, University Medical Center Groningen, Department of Pathology and Medical Biology Groningen, The Netherlands; h.i.heijink01@umcg.nl (I.H.H.), l.hesse@umcg.nl (L.H.)

[5] University of Groningen, University Medical Center Groningen, Department of Pulmonology, Groningen, The Netherlands; h.i.heijink01@umcg.nl (I.H.H.)

[6] Department of Gastroenterology and Hepatology, University of Groningen, University Medical Center Groningen, Groningen, The Netherlands; k.n.faber@umcg.nl (K.N.F.);

[7] Palm Beach Atlantic University, Lloyd L. Gregory School of Pharmacy, Department of Pharmaceutical Sciences, West Palm Beach, FL, USA; HARM_MAARSINGH@pba.edu (H.M.);

[8] German Center for Cardiovascular Research (DZHK), 20246 Hamburg, Germany, v.nikolaev@uke.de (V.O.N.).

* Correspondence: m.schmidt@rug.nl Tel.: +31503633322 (M.S.) orcid.org/0000-0003-3075-0630

Abstract: Epithelial-to-mesenchymal transition (EMT) plays a role in chronic obstructive pulmonary diseases (COPD). Cyclic adenosine monophosphate (cAMP) can inhibit transforming growth factor-β1 (TGF-β1) mediated EMT. Although compartmentalization via A-kinase anchoring proteins (AKAPs) is central to cAMP signaling, functional studies on their therapeutic value in the lung EMT process are lacking. Bronchial epithelial (BEAS-2B, primary HAE cells) were exposed to TGF-β1. Epithelial (E-cadherin, ZO-1) and mesenchymal markers collagen I (mRNA, protein) were analyzed. St-Ht31 disrupted AKAP-PKA interactions. TGF-β1 release was measured by ELISA. TGF-β1-sensitive AKAPs Ezrin, AKAP95 and Yotiao were silenced using siRNA. Cell migration was analyzed by wound healing assay, xCELLigence, Incucyte. Prior to TGF-β1, dibutyryl-cAMP (dbcAMP), fenoterol, rolipram, cilostamide, forskolin were used to elevate intracellular cAMP. TGF-β1 induced morphological changes, decreased E-cadherin but increased collagen I and cell migration, a process reversed by PF-670462. TGF-β1 altered (mRNA, protein) expression of Ezrin, AKAP95 and Yotiao. St-Ht31 decreased E-cadherin (mRNA, protein), but counteracted TGF-β1-induced collagen I upregulation. Cigarette smoke (CS) increased TGF-β1 release, activated TGF signaling, augmented cell migration and reduced E-cadherin expression, a process blocked by TGF-β1 neutralizing

Peer-reviewed version available at Cells 2020, 9, 356; doi:10.3390/cells9020356

antibody. Silencing of Ezrin, AKAP95 and Yotiao diminished TGF-β1-induced collagen I expression, as well as TGF-β1-induced cell migration. Fenoterol, rolipram, and cilostamide, in AKAP silenced cells pointed to distinct cAMP compartments. We conclude that Ezrin, AKAP95 and Yotiao promote TGF-β1-mediated EMT, linked to a TGF-β1 release by CS. AKAP members define the ability of fenoterol, rolipram and cilostamide to modulate the EMT process, and are potential relevant targets in the treatment of COPD.

Keywords: epithelial-to-mesenchymal transition; TGF-β1; cAMP; A-kinase anchoring protein; Ezrin; AKAP95; Yotiao; cigarette smoke; COPD

1. Introduction

Chronic obstructive pulmonary disease (COPD), which is primarily induced by cigarette smoke (CS), is characterized by irreversible airflow limitation that is linked to subepithelial airway fibrosis [1]. A vital player during organ fibrosis is epithelial-to-mesenchymal transition (EMT), a process in which epithelial cells gradually lose their epithelial phenotype and undergo transition to typical mesenchymal characteristics, featuring increased mitogenic capacity and enhanced extracellular matrix production [2-5]. Recent evidence suggests that EMT is involved in the fibrotic processes in the large and small airways during the pathogenesis of COPD as well as lung cancer [6-8]. Importantly, studies have provided evidence that EMT is an active process in the airways of smokers, particularly in those current-smoking COPD patients, indicating that CS-induced EMT contributes to COPD pathogenesis [6,7].

Transforming growth factor-β1 (TGF-β1) is another well-known inducer of EMT [5,9]. The cyclic adenosine monophosphate (cAMP) signaling pathway is one of multiple pathways that are implicated in the regulation of EMT [10-13]. A-kinase anchoring proteins (AKAPs) are a group of structurally diverse proteins localized at specific subcellular sites. They play a critical role in maintaining subcellular compartmentalization of cAMP by generating spatially discrete signaling complexes, which create local gradients of cAMP [14,15]. As scaffolding proteins, AKAPs bind protein kinase A (PKA) and a diverse subset of signaling enzymes, and thereby control cAMP microdomains in a spatio-temporal manner [5,16]. Studies have demonstrated that several AKAPs membranes are involved in TGF-β1-induced EMT *in vitro*. For instance, suppressing the expression of the AKAP family member Ezrin by small interfering RNA reduced both morphological changes and cell migration during TGF-β1-induced EMT in human alveolar A549 cells [17]. Knockdown by short hairpin RNA of another AKAP member Yotiao, also known as AKAP9, inhibited TGF-β1-induced EMT in colorectal cancer cells [18]. Additionally, AKAP9 interacts and co-localizes with E-cadherin at the cell membrane [19]. More importantly, silencing of AKAP9 reduced the functional epithelial barrier, suggesting the possibility of a specific role for AKAP9 in the maintenance of the epithelial barrier [19]. However, the function of AKAPs in regulating TGF-β1/ CS-induced EMT in human bronchial epithelial cells during is still unclear.

In the present study, we hypothesized that AKAPs could regulate TGF-β1/ CS-induced EMT in human bronchial epithelial BEAS-2B cells. We found that collagen I upregulation induced by TGF-β1 is diminished when AKAP-PKA interactions were disrupted by st-Ht31, whereas TGF-β1-induced E-cadherin downregulation was not reversed by st-Ht31, indicating that AKAPs are selectively involved in TGF-β1-induced collagen I increase. CS exposure increased TGF-β1 release

Peer-reviewed version available at Cells 2020, 9, 356; doi:10.3390/cells9020356

and activated TGF-β1 signaling pathway, which was able to be blocked by TGF-β1 neutralizing antibodies, therefore, contributing to EMT progression. We observed that mRNA and protein expression of the three AKAPs members Ezrin, Yotiao and AKAP95 was changed after TGF-β1 stimulation. The co-silencing of Ezrin, AKAP95 and Yotiao inhibited TGF-β1-induced cell migration in BEAS-2B cells and primary human airway epithelial cells. In addition, co-silencing of Ezrin, AKAP95 and Yotiao specifically accelerated the β_2-adrenergic receptor (β_2-AR)-induced reduction in TGF-β1-induced collagen I upregulation. Effects of cilostamide and rolipram were largely left unchanged pointing to AKAP defined cAMP sub-compartments.

2. Materials and Methods

2.1 Chemicals and antibodies

Recombinant human TGF-β1 protein was from R&D systems (Abingdon, UK). Fenoterol was purchased from Boehringer Ingelheim (Ingelheim, Germany). Rolipram, cilostamide, and bovine serum albumin (BSA) were from Sigma-Aldrich (St-Louis, MO, USA). Forskolin was from Tocris Bioscience (Bristol, UK). InCELLect™ AKAP St-Ht31 inhibitor peptide was purchased from Promega (Leiden, the Netherlands). Transfect reagent lipofectamine RNAiMax was purchased from Invitrogen (Bleiswijk, Netherlands). Control siRNA, Ezrin siRNA, AKAP95 siRNA and Yotiao siRNA were obtained from Santa Cruz Biotechnology (Heidelberg, Germany). All other chemicals were of analytical grade. The origin and dilution of the antibodies used are listed in Table 1.

Table 1. Antibodies used in western blotting and immunofluorescence

Antibody	Dilution	Company
Anti-E-cadherin	Western blotting,1:1,000 Immunofluorescence, 1:100	BD Biosciences
Anti-ZO-1	Immunofluorescence, 1:100	Invitrogen
Anti-type I collagen-UNLB	Western blotting, 1:1,000 Immunofluorescence, 1:20;	SouthernBiotech
Anti-α-SMA	Western blotting, 1:1,000	Sigma
Anti-Fibronectin	Western blotting, 1:1,000	Santa Cruz Biotechnology
Anti-Ezrin	Western blotting, 1:500	Abcam
Anti-AKAP95	Western blotting, 1:500	Santa Cruz Biotechnology
Anti-Yotiao	Immunofluorescence, 1:50	BD Biosciences
Anti-p-Smad2	Western blotting, 1:1,000	Cell Signaling Technology
Anti-p-Smad3	Western blotting, 1:1,000	Cell Signaling Technology
anti-total Smad2/3	Western blotting, 1:3,000	Santa Cruz Biotechnology
Anti-GAPDH	Western blotting, 1:10,000	Sigma

2.2 Cell culture

The human bronchial epithelial cell line BEAS-2B was maintained in RPMI 1640 supplemented with 10% v/v heat-inactivated fetal bovine serum (FBS) and antibiotics (penicillin 100 U/ ml, streptomycin 100 μg/ml) in a humidified atmosphere of 5% (v/v) CO_2 at 37°C. Cells were dissociated from T75 flasks with trypsin/EDTA and seeded in appropriate cell culture plates. Cells were maintained in 1%

v/v FBS medium 24 hours before and during stimulation, since a serum-free medium induced cell death.

Primary human airway epithelial (HAE) cells were isolated from residual tracheal and main stem bronchial tissue, from lung transplant donors post-mortem, within 1-8 h after lung transplantation, using the selection criteria for transplant donors according to the Eurotransplant guidelines. The tracheal tissue was collected in a Krebs–Henseleit buffer (composition in mM: NaCl 117.5, KCl 5.6, $MgSO_4$ 1.18, $CaCl_2$ 2.5, NaH_2PO_4 1.28, $NaHCO_3$ 25 and glucose 5.5) and primary HAE cells were collected by enzymatic digestion as described previously [20]. In short, airway epithelial cells were gently scraped off the luminal surface, washed once, and submerged cultured on petri-dishes which were pre-coated with a combination of fibronectin (10 μg/ml), bovine type I collagen (30 μg/ml), and bovine serum albumin (10 μg/ml) in PBS, using a keratinocyte serum free medium (Gibco, CA, USA) supplemented with 25 μg/ml bovine pituitary extract, 0.2 ng/ml epidermal growth factor and 1 μM isoproterenol for 4-7 days until they reached confluence, and then were trypsinized and seeded into 6-well plates for silencing experiments.

2.3 Cell stimulation

BEAS-2B cells were grown to confluence and then starved by exchange of complete medium to 1% v/v FBS medium for 24 hours. Cells were treated with 1 ng/ml, 3 ng/ml and 10 ng/ml for 24 hours, 48 hours and 72 hours. Based on gene and protein expression of EMT markers, 3 ng/ml TGF-β1 treatment for 24 hours was used in current study. Cells were pretreated for 30 minutes before stimulation with TGF-β1 for 24 hours with st-Ht31 (50 μM) to disrupt AKAP-PKA interaction [21] or with the casein kinase 1δ/ε inhibitor PF-670462 (1 and 10 μM) [22] to confirm that TGF-β1-induced EMT could be reversed in BEAS-2B cells. The β_2-agonist fenoterol (0.001– 10 μM), the phosphodiesterase (PDE)4 inhibitor rolipram (1 or 10 μM), the PDE3 inhibitor cilostamide (10 μM) and adenylyl cyclase agonist forskolin (10 μM) were added 30 minutes before 24 hours TGF-β1 stimulation. Different concentrations of CS extract were used to stimulate cells for 24 hours and supernatant was collected to measure TGF-β1 production by ELISA and to incubate basal BEAS-2B cells for 1 hour.

2.4 Transfection

Cells were grown to 80% confluence and were then transfected using lipofectamine RNAiMax reagent in a 1:1 reagent: siRNA ratio in complete growth medium without antibiotics. Cells were transfected with 40 nM control siRNA, 40 nM Ezrin siRNA, 40 nM AKAP95 siRNA and 40 nM Yotiao siRNA for 48 hours before TGF-β1 treatment. After TGF-β1 treatment for 24 hours, the cells were lysed for real-time quantitative PCR and western blotting analysis.

2.5 Real-time quantitative PCR

Total RNA was extracted from cells using the Maxwell 16 LEV simplyRNA Tissue Kit (Promega, Madison, WI, USA) according to the manufacturer's instructions. The total RNA yield was determined by NanoDrop 1000 Spectrophotometer (Thermo Fisher Scientific, Wilmington, DE, USA). Equal amounts of RNA were used to synthesize cDNA. An Illumina Eco Real-Time PCR system was used to perform real-time qPCR experiments. PCR cycling was performed with denaturation at 94 °C for 30 sec, annealing at 59 °C for 30 sec and extension at 72 °C for 30 sec for 45 cycles. RT-qPCR data

was analyzed by LinRegPCR software [23]. To analyze RT-qPCR data, the amount of target gene was normalized to the reference genes 18S ribosomal RNA, SDHA and RPL13A. Primer sequences are listed in Table 2.

Table 2. Primer sequences

Primers	Species	Forward sequence 5′- 3′	Reverse sequence 5′- 3′
18s	Homo sap.	CGCCGCTAGAGGTGAAATTC	TTGGCAAATGCTTTCGCTC
SDHA	Homo sap.	GGGAAGACTACAAGGTGCGG	CTCCAGTGCTCCTCAAAGGG
RPL13A	Homo sap.	ACCGCCCTACGACAAGAAAA	GCTGTCACTGCCTGGTACTT
E-cadherin	Homo sap.	TGCCCAGAAAATGAAAAAGG	GTGTATGTGGCAATGCGTTC
Collagen 1α1	Homo sap.	AGCCAGCAGATCGAGAACAT	TCTTGTCCTTGGGGTTCTTG
AKAP1	Homo sap.	CCAGTGCAGGAGGAAGAGTATG	CTCCCTCGACACCTCTATCCT
AKAP5	Homo sap.	GACGCCCTACGTTGATCT	GAAATGCCCAGTTTCTCTATG
AKAP11	Homo sap.	CCGGGCTAGTTCTGAATGGG	TGCTCCGACTTCACATCCAC
AKAP12	Homo sap.	CAAGCACAGGAGGAGTTACAG	CTGGTCTTCCAAACAGACAATG
AKAP95	Homo sap.	ATGCACCGACAATTCCGACT	CATAGGACTCGAACGGCTGG
Yotiao	Homo sap.	AACCTGAAGATGTGCCTCCTG	CTGGAGTGCATACCTTTC
Ezrin	Homo sap.	GCTTTTTGATCAGGTGGTAAAGACT	TCCACATAGTGGAGGCCAAAGT

2. 6 Western blotting

Cells were lyzed in a lysis buffer and homogenized protein concentration was measured by BCA protein assay (Pierce). Equal amounts of the total proteins were loaded into 10% SDS–polyacrylamide gel electrophoresis. After being transferred to a nitrocellulose membrane, membranes were blocked with Roti-Block (Carl Roth, Karlsruhe, Germany). Primary antibodies (**Table 1**) were incubated at 4°C overnight, followed by a secondary antibody (anti-mouse IgG, 1: 5,000, anti-rabbit IgG, 1: 5,000 or anti-goat IgG, 1:5000, Sigma) incubation at room temperature for two hours. Protein bands were developed on film using a Western detection ECL-plus kit (PerkinElmer, Waltman, MA). ImageJ software was used for band densitometry analysis.

2.7 Immunofluorescence

50,000 cells were seeded on coverslips (12 mm) and stimulated with different reagents for a certain period as described previously. Then, the cells were fixed with 1:1 methanol/acetone in at -20°C for 20 minutes. After 3 times washing with PBS, the cells were then blocked using 1% (w/v) BSA/PBS with 2% donkey serum for one hour. Primary antibodies (**Table 1**) were applied overnight at 4°C, after which secondary antibody Alexa Fluor 488 nm donkey anti-goat and Cy™3 AffiniPure donkey anti-mouse (Jackson, Cambridgeshire, UK) were incubated for 2 hours. Finally, slides were mounted with a mounting medium containing DAPI (Abcam, Cambridge, UK). Images were captured with a Leica DM4000b Fluorescence microscope (Leica Microsystems, Germany) equipped with a Leica DFC 345 FX camera.

2.8 Cigarette smoke extract (CSE) preparation

CSE preparation was prepared as previously described [21]. Two 3R4F research cigarettes (University of Kentucky, Lexington, USA) without a filter were combusted into 25 ml 1% v/v FBS medium using a peristaltic pump (45 rpm, Watson Marlow 323E/D, Rotterdam, The Netherlands).

This medium was designated as 100% CSE and was diluted to certain concentrations in different experiments.

2.9 Wound healing assay

Cells were grown to confluence and were scratched with a pipette tip. After being washed once to remove the detached cells, cells were allowed to migrate into the wound area in the absence or presence of TGF-β1 and different siRNAs. The wound area was photographed immediately after a scratch and then after 24 hours of stimulation.

2.10 xCELLigence transwell migration

Cell migration was further tested using the label-free and real-time xCELLigence transwell migration system CIM-16 plates (RTCA DP, ACEA Biosciences, San Diego, CA). A 10% v/v FBS growth medium was applied as a chemoattractant in the lower chamber. 25 µl of 1% v/v FBS medium was added to the top chamber and plates were placed in the system for equilibration. Cells were passaged and 90,000 cells were seeded on the top chamber in 1% v/v FBS medium containing TGF-β1 or CS extract. Cells were then placed back in the system for future monitoring for 24 hours at 37°C in a 5% (v/v) CO_2 humidified atmosphere. The system was set to take a cell index measurement at 15 min intervals.

2.11 Incucyte

BEAS-2B cells were transduced with NucLight Red lentivirus (Essen Bioscience, Ann Arbor, MI) to produce red fluorescent proteins which label the BEAS-2B cell nucleus according to the product instruction. Red-labeled BEAS-2B cells (10,000 per well) were plated on 96-well ImageLock cell migration plates (Essen Bioscience, Ann Arbor, MI) and incubated overnight. After silencing with a combination of Ezrin, AKAP95 and Yotiao siRNA, the cell monolayer was scratched with a 96-pin WoundMaker (Essen Bioscience), and the cells washed with PBS (phosphate-buffered saline) before adding 3 ng/ml TGF-β1 or diluted CS extract. Cell migration and proliferation were monitored by a microscope gantry inside a cell incubator, which was connected to a networker external controller hard drive that gathered and processed image data (Incucyte, Essen Bioscience, Ann Arbor, MI).

2.12 Statistics

All data were analyzed by GraphPad Prism (GraphPad Software, Inc.) and expressed as mean ± SEM. At least 3 independent experiments were conducted for each treatment. The exact repeats are indicated in the figure legends. Normal data distribution was determined by Shapiro-Wilk test. The statistical significance was performed using unpaired Student's t-test or ANOVA test for multiple comparisons. For non-Gaussian distributed data, the significance was determined using a non-parametric one-way ANOVA with a *post hoc* Kruskal-Wallis multiple comparisons test. $P < 0.05$ was considered statistically significant.

3. Results

3.1 Effect of TGF-β1 on cell morphology and phenotype markers in BEAS-2B cells

Peer-reviewed version available at Cells 2020, 9, 356; doi:10.3390/cells9020356

As shown in **Fig. 1A,** TGF-β1 stimulation for 24 hours changed the morphology of BEAS-2B cells from a typical epithelial shape to an elongated and spindle-like morphology. The mRNA expression of *E-cadherin* was significantly decreased in TGF-β1 stimulated cells compared to the control cells, whereas TGF-β1 dramatically up-regulated *collagen I* mRNA expression **(Fig. 1B)**. Protein levels of multiple epithelial and mesenchymal markers were analyzed by western blotting, including collagen I, fibronectin, and α-smooth muscle actin (α-SMA) (**Fig. 1C**). Following the effect of mRNA levels, TGF-β1 strongly decreased E-cadherin, while increasing collagen I protein levels (**Fig. 1C**). Signals of fibronectin and α-SMA were weaker and more variable compared to collagen I. Thus, collagen I and E-cadherin were from this point used as markers for the mesenchymal and epithelial phenotype makers, respectively. In addition, immunofluorescence images showed that the protein expression of another epithelial marker ZO-1 was significantly decreased after TGF-β1 stimulation, whereas collagen I protein expression was clearly enhanced **(Fig. 1D)**. The immunofluorescent staining of E-cadherin was not as obvious as that of ZO-1, however, a clear decrease in the protein expression of E-cadherin was observed after TGF-β1 stimulation **(Fig. 1D)**.

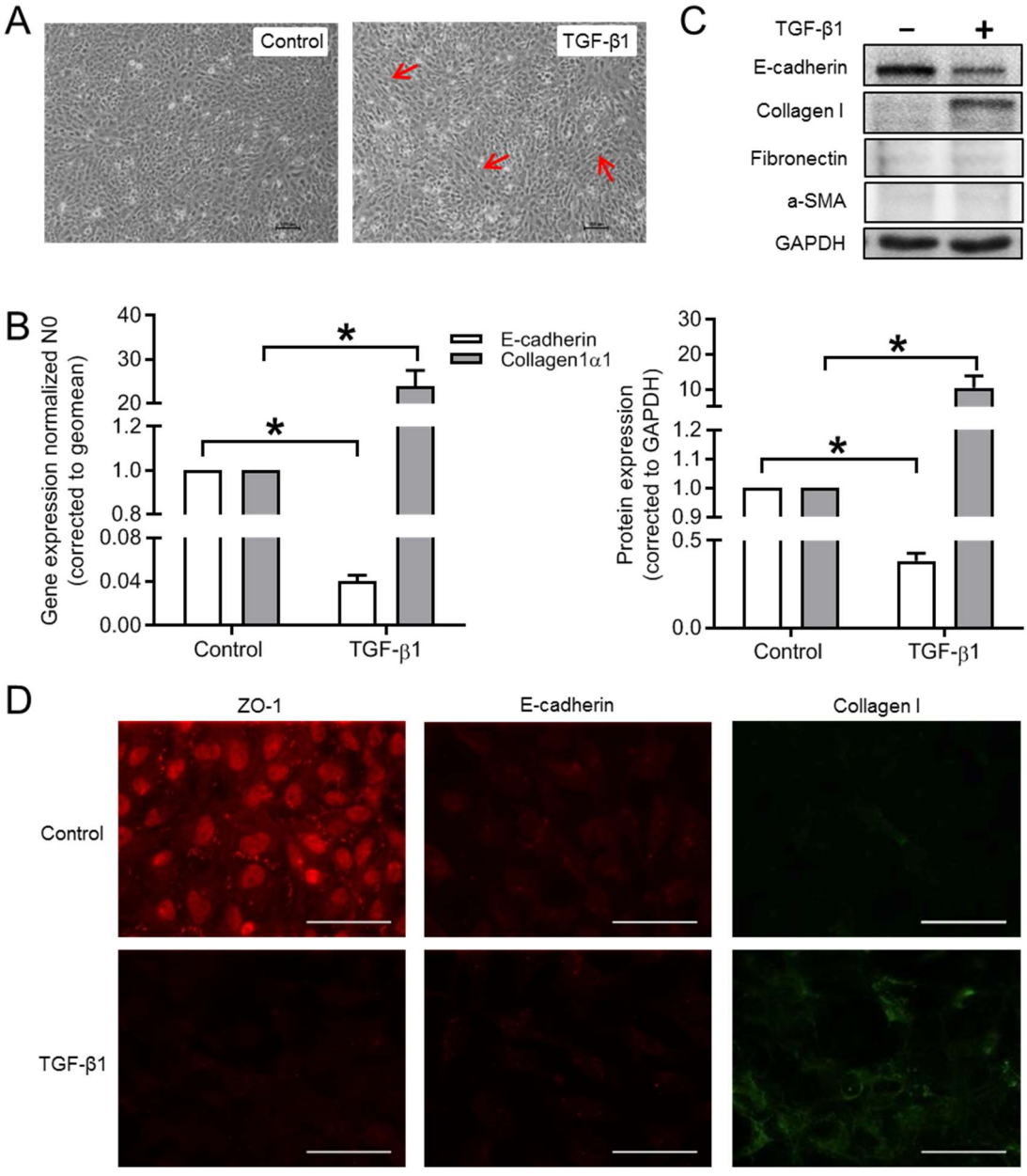

Peer-reviewed version available at Cells 2020, 9, 356; doi:10.3390/cells9020356

Figure 1. Effects of TGF-β1 on cell morphology and EMT markers. (A) Morphological changes of BEAS-2B cells after stimulated with TGF-β1 (3 ng/ml) for 24 hours. Spindle-like cells were indicated with red arrow. (B-C) Gene (B) and protein (C) expressions of E-cadherin and collagen I were analyzed in BEAS-2B cells with or without TGF-β1 stimulation using real-time quantitative PCR and western blotting, respectively. Representative western blotting images of E-cadherin and collagen I were shown in figure C. (D) Immunofluorescence images of ZO-1, E-cadherin and collagen I after 24 hours stimulation of TGF-β1. Scale bar represents 100 μm. Data represent 3-6 independent experiments. Data are expressed as mean ± SEM, *: $p<0.05$; significant difference between indicated groups.

3.2 Disruption of AKAP-PKA interaction diminishes TGF-β1-induced collagen I upregulation

To determine the role of the physical interaction between AKAP and PKA in the TGF-β1-induced EMT, the effect of the cell-permeable PKA-anchoring disruptor peptide, st-Ht31, on gene and protein expression of EMT markers was examined. As shown in **Fig. 2A**, treatment with 50 μM st-Ht31 alone significantly decreased *E-cadherin* gene expression and this effect was even more pronounced at the protein level **(Fig. 2C)**.

Surprisingly, st-Ht31 pre-treatment did not prevent the TGF-β1-induced downregulation of E-cadherin **(Fig. 2A, 2C)**. In contrast, st-Ht31 significantly decreased collagen I protein expression in TGF-β1-stimulated cells **(Fig. 2D)**, leaving mRNA levels unchanged **(Fig. 2B)**.

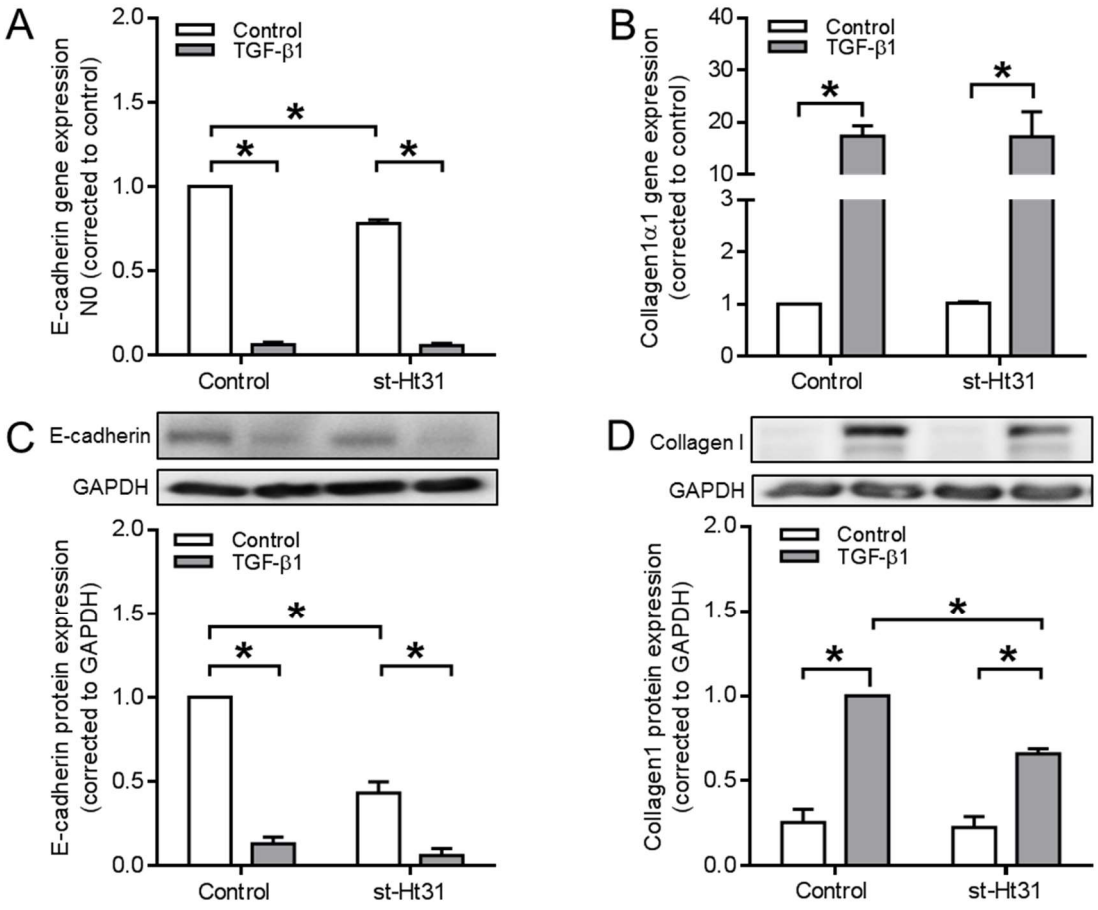

Peer-reviewed version available at Cells 2020, 9, 356; doi:10.3390/cells9020356

Figure 2. Role of st-Ht31 on EMT markers in BEAS-2B cells. BEAS-2B cells were pre-incubated with 50 μM st-Ht31 for 30 minutes, following stimulated with 3 ng/ml TGF-β1 for 24 hours. Gene (A, C) and protein (B, D) expressions of E-cadherin (A-B) and collagen I (C-D) were examined using real-time quantitative PCR and western blotting, respectively. Data represent 3 independent experiments. Data are expressed as mean ± SEM, *: p<0.05; significant difference between indicated groups.

3.3 CSE activates TGF-β1 signaling pathway

It has been demonstrated that cigarette smoke (CS) exposure induces TGF-β1 release [6,24] an may therefore contribute to EMT in lung epithelial cells. Indeed, we confirmed that CSE exposure significantly increases TGF-β1 release by BEAS-2B cells used in this study **(Fig. 3A)**. Moreover, phosphorylation of SMAD2 **(Fig. 3B)** and SMAD3 (data not shown) was increased by CSE exposure. To confirm that CSE-induced EMT depends on TGF-β1 release we next used TGF-β neutralizing antibodies to block TGF-β1 signaling. A 24 h exposure of BEAS-2B cells to 1% CSE significantly decreased E-cadherin protein levels, which was reversed when TGF-β neutralizing antibodies were added 30 minutes prior the TGF-β challenge **(Fig. 3C)**. To test whether the TGF-β1-induced E-cadherin decrease could be modulated in BEAS-2B cells, these cells were exposed to a selective inhibitor of the δ- and ε-isoforms of casein kinase I, PF-670462, as it was shown before to reverse TGF-β1-induced EMT in A549 cells [22]. Indeed, pretreatment of BEAS-2B cells with PF-670462 dose-dependently prevented TGF-β1-induced E-cadherin loss and collagen I gain **(Fig. 3E-F)**.

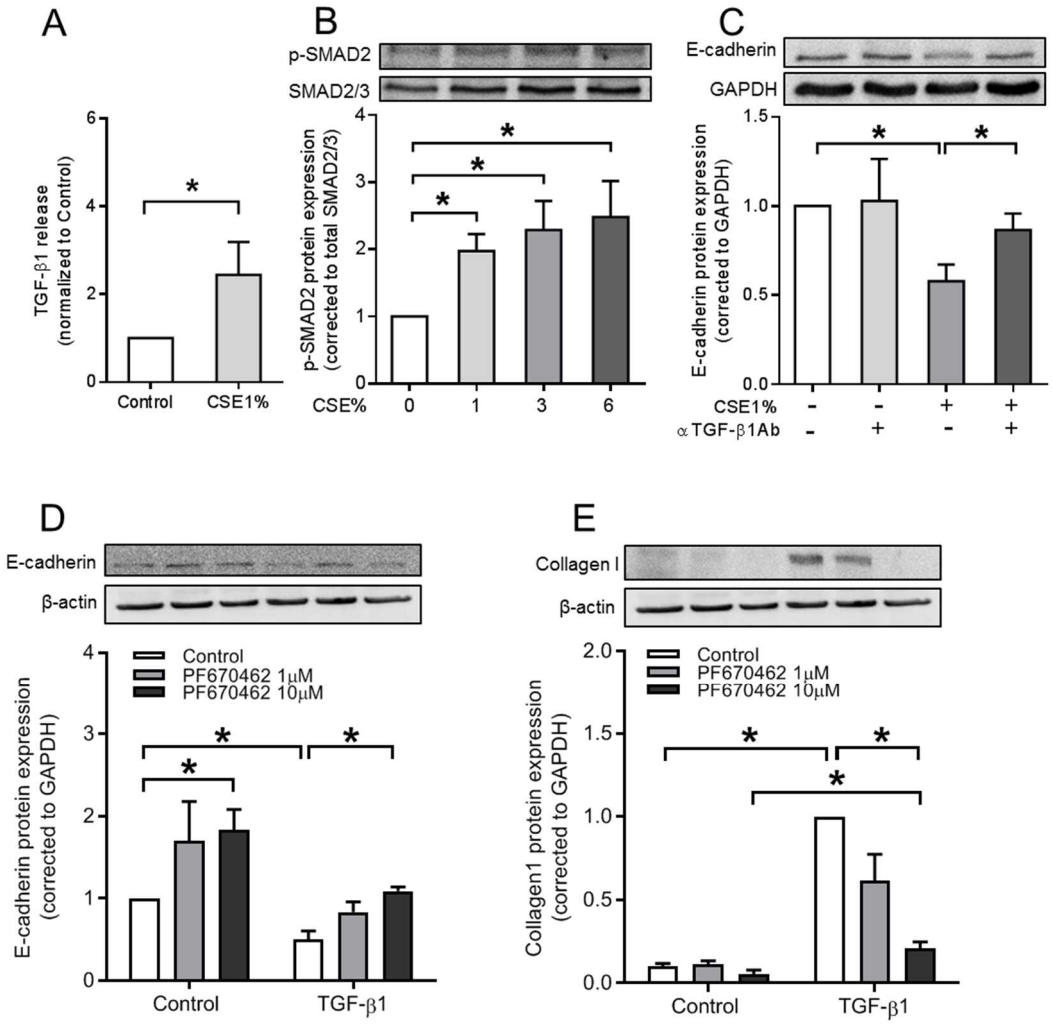

Figure 3. The effect of CS extract on TGF-β1 release, TGF-β1 signaling and TGF-β1 induced EMT in BEAS-2B cells. Effect of the δ/ε casein kinase I isoform inhibitor PF-670462. (A) TGF-β1 release was measured by ELISA using the supernatant after 24 hours 1% CSE exposure. (B) Representative western blotting images and quantification of phospho-SMAD2 in BEAS-2B cells treated with 24 hours CS extract-incubated medium for 1 hour. (C) BEAS-2B cells were pre-incubated with 10 ng/ml TGF-β neutralizing antibody for 30 minutes, following stimulated with 1% CSE for 24 hours. Representative western blotting images and quantification of E-cadherin were shown. BEAS-2B cells were pre-incubated with 1 μM or 10 μM PF670462 for 30 minutes, following stimulated with 3ng/ml TGF-β1 for 24 hours. Protein (D-E) expressions of E-cadherin (D) and collagen I (E) were examined by western blotting. Data represent 3-6 independent experiments. Data are expressed as mean ± SEM, *: $p<0.05$; significant difference between indicated groups.

3.4 Ezrin, AKAP95 and Yotiao are involved in TGF-β1-induced EMT

Next we studied which member(s) of the AKAP family exert sensitivity to TGF-β1 in BEAS-2B cells. TGF-β1 selectively and significantly down-regulated the mRNA levels of *Ezrin*, whereas the mRNA expression of *AKAP95* and *Yotiao* was enhanced. *AKAP1*, *AKAP5*, *AKAP11* and *AKAP12* mRNA levels were not affected by TGF-β1 **(Fig. 4A)**. We observed an increase in AKAP95 protein, but not Ezrin **(Fig. 4B)**. Immunofluorescence microscopy staining showed that TGF-β1 significantly increased the protein expression of Yotiao **(Fig. 4C)**.

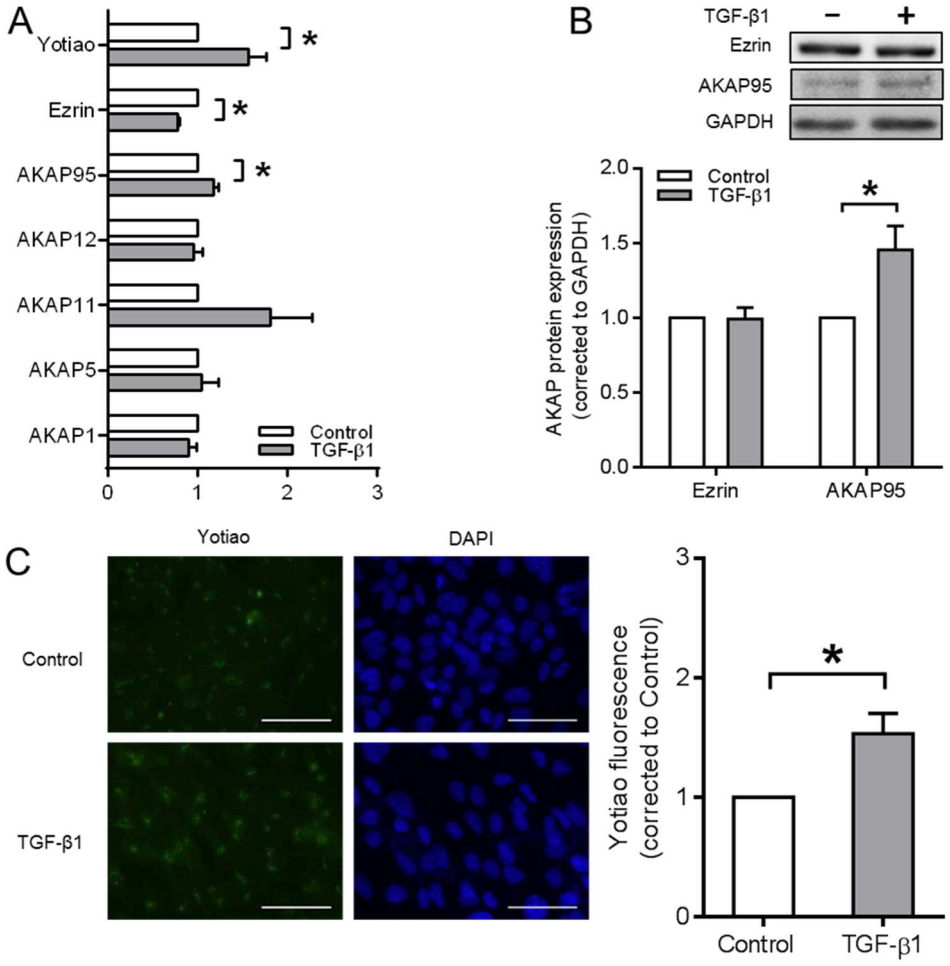

Figure 4. Effect of TGF-β1 on gene and protein expression of AKAPs in BEAS-2B cells. (A) Gene expressions of *AKAP1, AKAP5, AKAP11, AKAP12, AKAP95, Ezrin and Yotiao* were studied by real-time quantitative PCR. (B) Representative western blotting images and quantification of Ezrin and AKAP95. (C) Immunofluorescence images of Yotiao after 3 ng/ml TGF-β1 stimulation for 24 hours. Scale bar represents 100 μm. Data represent 5-7 independent experiments. Data are expressed as mean ± SEM, *: $p<0.05$; significant difference between indicated groups.

Since TGF-β1 modulated the expression of Ezrin, AKAP95 and Yotiao, we hypothesized that these factors might be involved in TGF-β1-induced EMT. To study this, we silenced the expression of Ezrin, AKAP95 and Yotiao in BEAS-2B cells using small interfering RNAs (siRNA). Real-time quantitative PCR confirmed the siRNA-mediated reduction of *Ezrin*, *AKAP95* and *Yotiao* (29.4 ± 7.4%, 34.4 ± 6.8%; and 43.4 ± 15.3%, respectively;), which was accompanied with similar reductions in the corresponding proteins (Ezrin, 25.1 ± 0.1%; AKAP95 51.2 ± 3.7%; **Supplementary Fig. S1**). We observed 40% and 63% decreased E-cadherin protein levels in Ezrin- or AKAP95-silenced cells, respectively, an effect which was even more pronounced in TGF-β1-treated cells **(Fig. 5A, Table 3**). Silencing of Yotiao did not reduce the E-cadherin expression **(Fig. 5A)**. Silencing of Ezrin, AKAP95 or Yotiao suppressed the TGF-β1-induced upregulation of the mesenchymal maker collagen I by about 40% **(Fig. 5B, Table 3)**. We then questioned whether co-silencing of Ezrin, AKAP95 and Yotiao would further alter the expression of the EMT markers. Co-silencing of all 3 factors (siM) reduced the protein levels of E-cadherin after TGF-β1 stimulation to 11% **(Fig. 5C, Table 3)**, as compared to ~40% when the factors were silenced individually **(Fig. 5A)**. More importantly, collagen I protein levels were reduced to 25% after triple-silencing in TGF-β1-stimulated cells when compared to ~60% after single-silencing **(Fig. 5D**, compared to **Fig 5B**, **Table 3)**. We therefore performed the next experiments in cells with co-silenced Ezrin, AKAP95 and Yotiao.

Preprints (www.preprints.org) | NOT PEER-REVIEWED | Posted: 31 October 2019 doi:10.20944/preprints201910.0358.v1

Peer-reviewed version available at Cells 2020, 9, 356; doi:10.3390/cells9020356

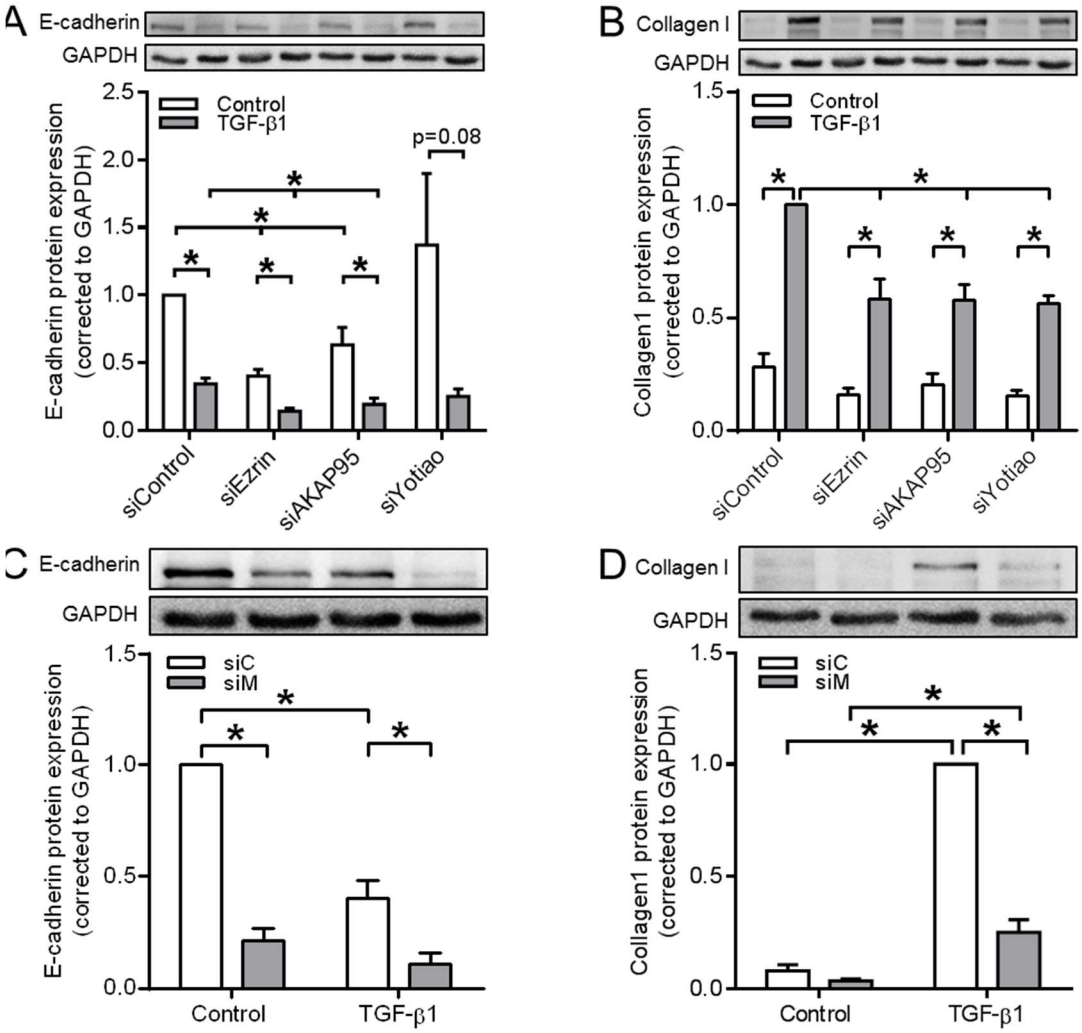

Figure 5. Silencing of Ezrin, AKAP95 and Yotiao diminished TGF-β1-induced collagen I upregulation. (A-B) Representative western blotting images and quantification of E-cadherin (A) and collagen I (B) in cells transfected with the siRNA of Ezrin, AKAP95 or Yotiao in combination with TGF-β1 treatment. (C-D) Representative western blotting images and quantification of E-cadherin (C) and collagen I (D) in cells transfected with a combination siRNA of Ezrin, AKAP95 and Yotiao together with TGF-β1 treatment. Data represent 4-6 independent experiments. Data are expressed as mean ± SEM, *: $p<0.05$; significant difference between indicated groups.

Table 3. The comparison of E-cadherin and Collagen I protein expression in signal and multiple AKAPs silencing and the pretreatment of st-Ht31.

Treatment	E-cadherin		n	Treatment	Collagen I		n
	-TGF-β1	+TGF-β1			-TGF-β1	+TGF-β1	
siControl	1.00±0.00	0.35±0.04	6	siControl	0.28±0.06	1.00±0.00	6
siEzrin	0.40±0.05	0.14±0.02	6	siEzrin	0.16±0.03	0.58±0.09	6
siAKAP95	0.63±0.13	0.19±0.05	6	siAKAP95	0.20±0.05	0.58±0.07	6
siYotiao	1.37±0.53	0.25±0.06	4	siYotiao	0.15±0.02	0.56±0.04	4

siControl	1.00±0.00	0.40±0.08	5	siControl	0.08±0.03	1.00±0.00	5
siMultiple	0.21±0.06	0.11±0.05	5	siMultiple	0.04±0.01	0.25±0.06	5
Control	1.00±0.00	0.13±0.02	3	Control	0.26±0.08	1.00±0.00	3
st-Ht31	0.43±0.04	0.06±0.02	3	st-Ht31	0.23±0.06	0.66±0.03	3

3.5 Ezrin, AKAP95 and Yotiao are required for TGF-β1-induced cell migration

As expected, TGF-β1 stimulation increased BEAS-2B cell motility compared to control cells, as analyzed in scratch assays **(Fig. 6A-B)**. Co-silencing of Ezrin, AKAP95 and Yotiao profoundly reduced cell migration and normalized cell migration of TGF-β1-stimulated cells back to control levels **(Fig. 6A-B)**. In a real time assay for cell migration using the xCELLigence platform, TGF-β1 increased cells migration in the early phase, which was reduced in cells co-treated with the siRNA of Ezrin, AKAP95 and Yotiao, even though no significance was observed (data not shown). Additionally, cell migration was also monitored by another real-time system Incucyte. The migration of cells with co-silenced Ezrin, AKAP95 and Yotiao upon wounding was significantly slowed down both at baseline and upon treatment with TGF **(Fig. 6C)**. In silenced cells, TGF-β1 increased cell migration was significantly slower compared to cells. Additionally, we found that the cell proliferation within 24 hours in each treatment was quite limited, indicating that the wound closure was due to migration instead of proliferation **(Fig. 6D)**. Even though the effects were much less pronounced and more variable, we found that CSE exposure enhanced cell migration in the early phase, which was examined by xCELLigence transwell system. Co-silencing of Ezrin, AKAP95 and Yotiao tended to decrease CS-induced cell migration, even though no significance was observed (data not shown). The effect of CS extract exposure on activating cell migration was further confirmed by the real time monitoring system Incucyte **(Supplementary Fig. S2 A-B)**.

Preprints (www.preprints.org) | NOT PEER-REVIEWED | Posted: 31 October 2019 doi:10.20944/preprints201910.0358.v1

Peer-reviewed version available at Cells 2020, 9, 356; doi:10.3390/cells9020356

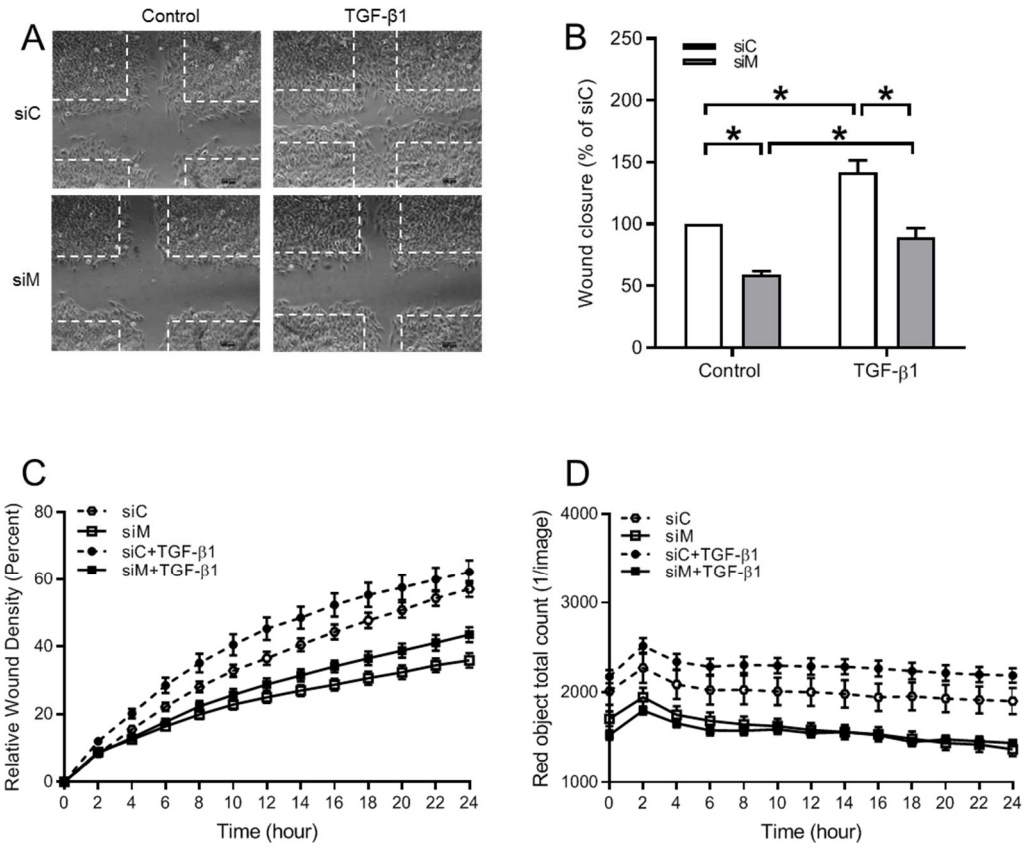

Figure 6. Role of Ezrin, AKAP95 and Yotiao in TGF-β1-induced cell migration using BEAS-2B cells. (A) Representative images of wound healing assay of BEAS-2B cells after 24 hours post scratch. The white dotted line indicated borders of scratches at 0 hour. (B) Quantification of wound closure of TGF-β1 treated cells in co-cultured with combined knockdown of Ezrin, AKAP95 and Yotiao. (C) Cell migration was monitored every two hours in a 96-well plate using a real time system Incucyte. (D) Cell proliferation was monitored by Incucyte. Data represent 3-5 independent experiments. Data are expressed as mean ± SEM, *: $p<0.05$; significant difference between indicated groups.

3.6 The role of AKAPs in primary HAE cells

To translate our findings obtained using the BEAS-2B cells to clinically more relevant cell types, we applied identical treatments to primary human airway epithelial (HAE) cells. As shown in **Fig. 7A**, even though the measures did not reach significance, TGF-β1 tended to change the expression of *Yotiao*, *Ezrin*, *AKAP12*. In addition, we found that TGF-β1 was able to decrease cell-cell interaction, which was observed in immunofluorescence staining of ZO-1 **(Fig. 7B)**. Additionally, to confirm the findings in BEAS-2B cells, we also investigated whether silencing three AKAP genes could affect the cell migration using primary HAE cells. As shown in **Fig. 7C**, similar results were observed in primary HAE cells, even though the overall migration in primary HAE cells was much less compared with that in BEAS-2B cells. Importantly, in cells silenced Ezrin, AKAP95 and Yotiao, TGF-β1 was no long able to promote cell migration. Of note was that in primary epithelial cells silencing of the TGF-β1 sensitive AKAPs did not interfere with the basal migration capacity.

Preprints (www.preprints.org) | NOT PEER-REVIEWED | Posted: 31 October 2019 doi:10.20944/preprints201910.0358.v1

Peer-reviewed version available at Cells 2020, 9, 356; doi:10.3390/cells9020356

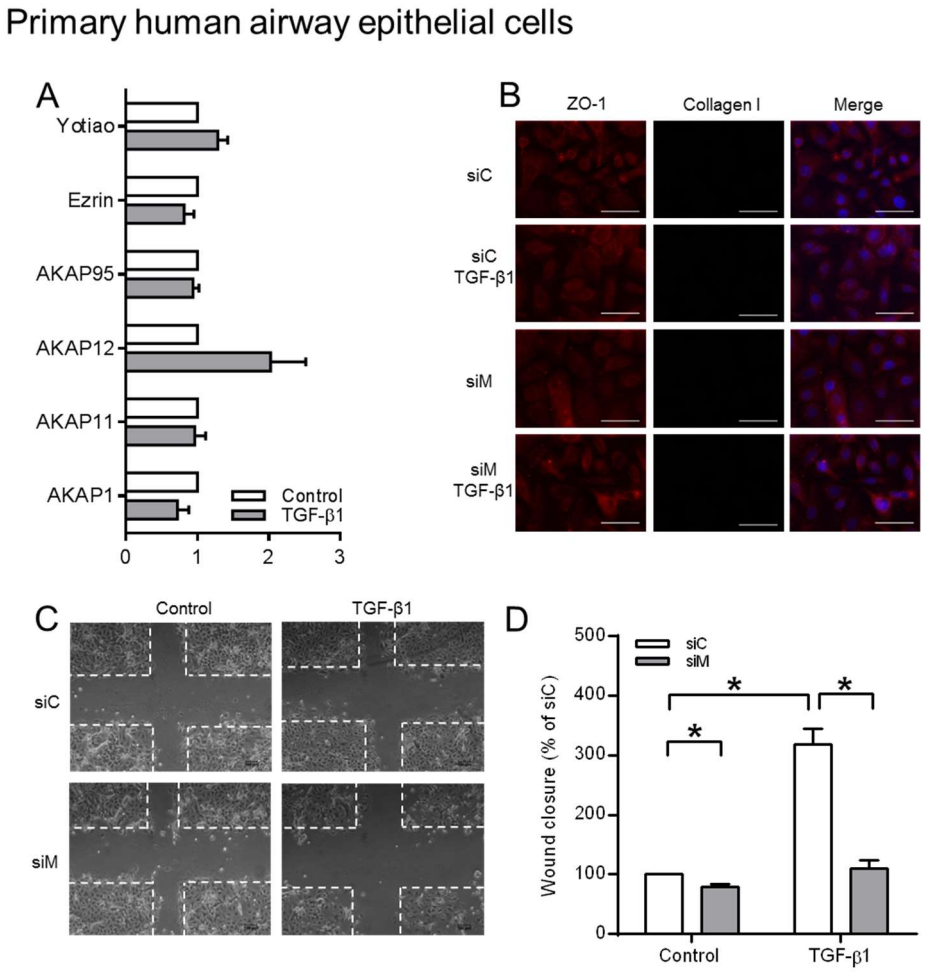

Figure 7. The effect of TGF-β1 on AKAPs expression and role of Ezrin, AKAP95 and Yotiao in TGF-β1-induced cell migration using pHAE cells. (A) Gene expressions of *AKAP1, AKAP11, AKAP12, AKAP95, Ezrin and Yotiao* were studied by real-time quantitative PCR. (B) Representative immunofluorescence images of EMT markers in pHAE cells after TGF-β1 stimulation for 24 hours. (C) Representative images of wound healing assay after 24 hours post scratch. The white dotted line indicated borders of scratches at 0 hour. (D) Quantification of wound closure of TGF-β1 treated cells in co-cultured with combined knockdown of Ezrin, AKAP95 and Yotiao. Data represent 5 independent experiments. Data are expressed as mean ± SEM, *: $p<0.05$; significant difference between indicated groups.

3.7 cAMP donors decrease TGF-β1-induced collagen I upregulation

To further study the role of compartmentalized cAMP, the cell-membrane permeable cAMP derivative dbcAMP was used to disrupt cAMP compartmentalization in BEAS-2B cells. We found that dbcAMP does-dependently increased the protein expression of epithelial marker E-cadherin in control BEAS-2B cells, without affecting the reduced levels of E-cadherin in TGF-β1-treated cells **(Fig. 8A)**. In contrast, TGF-β1-induced collagen I upregulation was significantly decreased by dbcAMP in a dose dependent manner, while leaving the basal levels unaffected **(Fig. 8B)**. Immunofluorescence microscopy analyses revealed that dbcAMP slightly reduced the basal expression of ZO-1 in BEAS-2B cells, while leaving the TGF-β1-induced reduction largely unaffected **(Fig. 8C-D)**. Moreover, TGF-

Peer-reviewed version available at Cells 2020, 9, 356; doi:10.3390/cells9020356

β1-induced collagen I expression was reduced by dbcAMP in these cells, without affecting basal levels **(Fig. 8C-D)**.

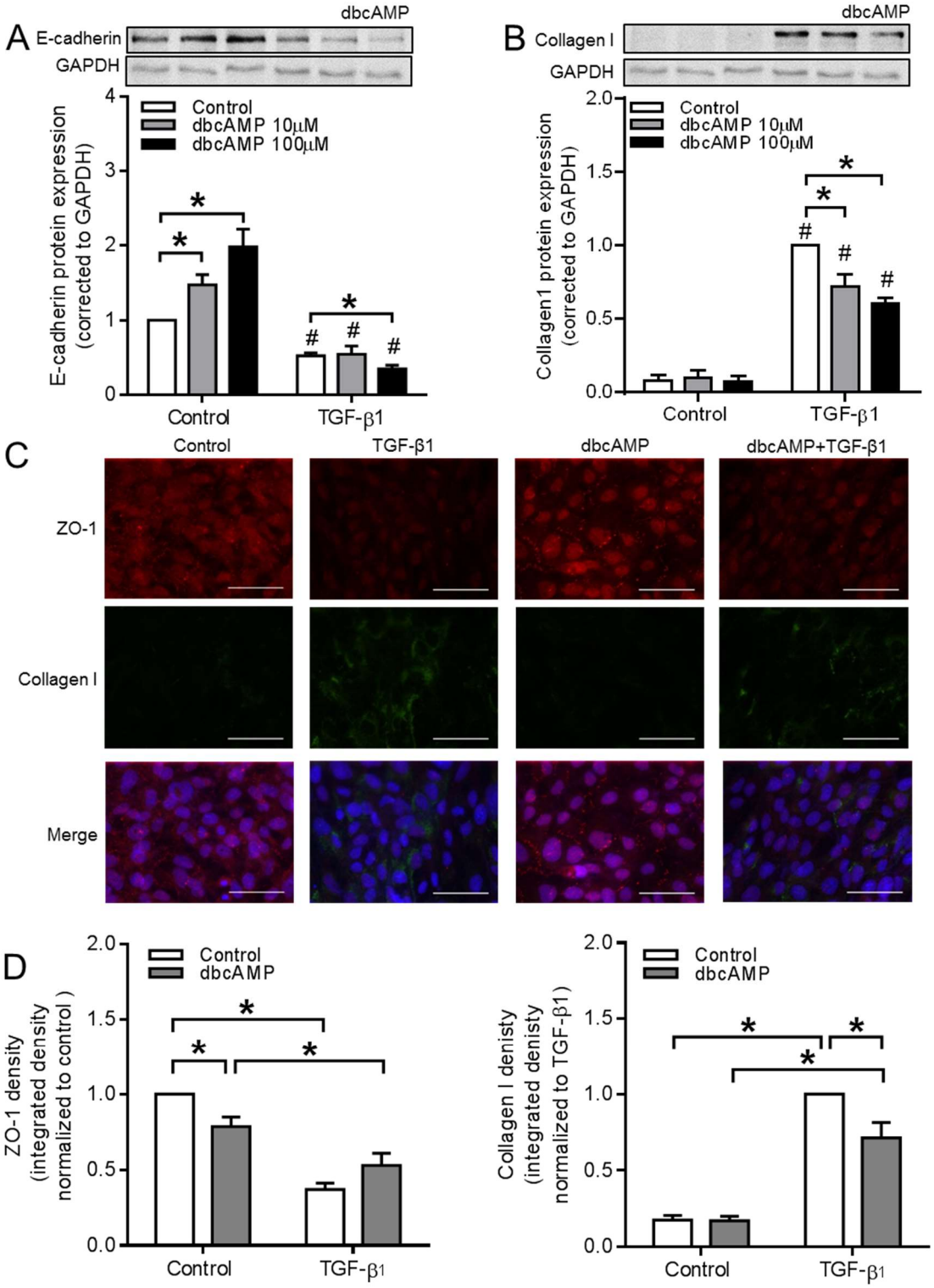

Figure 8. Effect of dbcAMP on TGF-β1-induced EMT markers expression in BEAS-2B cells. (A-B) protein expressions of E-cadherin (A) and collagen I (B) were analyzed in BEAS-2B cells pre-incubated with 10μM or 100μM dbcAMP for 30 minutes before TGF-β1 stimulation. (C-D) Immunofluorescence images (C) and quantification (D) of ZO-1 and collagen I after TGF-β1 stimulation for 24 hours. Scale bar represents 100μm. Data represent 4-6 independent experiments.

Peer-reviewed version available at Cells 2020, 9, 356; doi:10.3390/cells9020356

Data are expressed as mean ± SEM, *: p<0.05; significant difference between indicated groups; #: p<0.05; significant difference between with or without TGF-β1 treatment.

To further evaluate if cAMP compartmentalization contributed to the EMT process in our model, the effect of the β_2-agonist fenoterol, the PDE4 inhibitor rolipram, the PDE3 inhibitor cilostamide, and the adenylyl cyclase activator forskolin were studied. Although none of these compounds affected basal levels of E-cadherin or the reduction induced by TGF-β1 **(Fig. 9A, 9C)**, they each suppressed TGF-β1-induced collagen I upregulation **(Fig. 9B, 9D).**

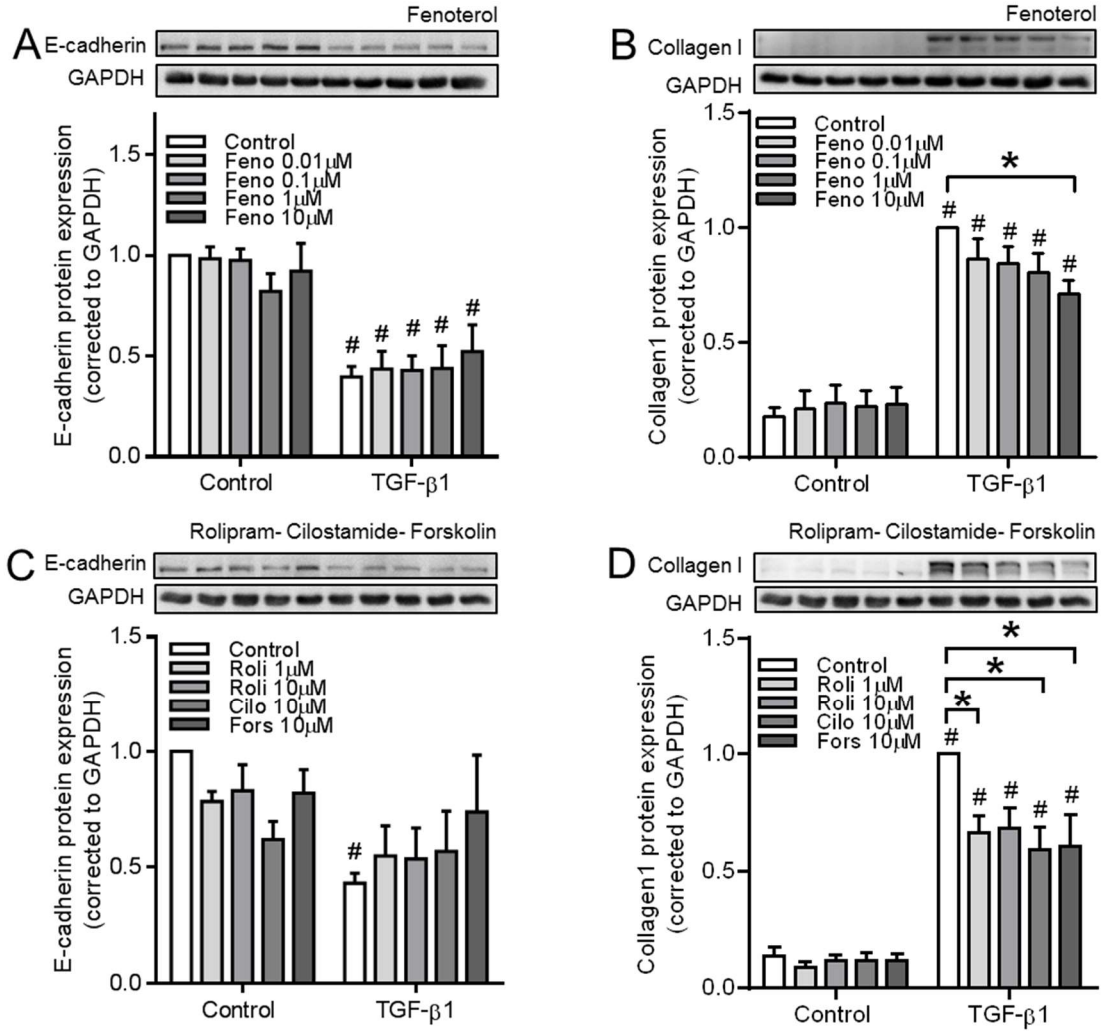

Figure 9. Effect of fenoterol, rolipram, cilostamide and forskolin on TGF-β1-induced EMT makers using BEAS-2B cells. (A-D) Representative western blotting images and quantification of E-cadherin (A, C) and collagen I (B, D) in cells pre-incubated with fenoterol (A-B) or rolipram, cilostamide and forskolin (C-D) before TGF-β1 treatment. Data represent 5-6 independent experiments. Data are expressed as mean ± SEM, *: p<0.05; significant difference between indicated groups. #: p<0.05; significant difference between with or without TGF-β1 treatment.

3.8 Ezrin, AKAP95 and Yotiao differentially contribute to cAMP compartments

In order to study to which extent defined cAMP compartments might contribute to the TGF-β1-induced EMT process in BEAS-2B cells, we tested the effects of fenoterol, rolipram and cilostamide

Preprints (www.preprints.org) | NOT PEER-REVIEWED | Posted: 31 October 2019 doi:10.20944/preprints201910.0358.v1

Peer-reviewed version available at Cells 2020, 9, 356; doi:10.3390/cells9020356

in Ezrin-AKAP95-Yotiao (siM) co-silenced cells. We found that fenoterol further decreased siM-induced collagen I downregulation from 54.5 ± 9.1% to 24.9 ± 8.0% **(Fig. 10A, Table 4)**. On the contrary, rolipram and cilostamide were unable to further reduce collagen I protein expression **(Fig. 10B-C, Table 4)**, indicating that Ezrin, AKAP95 and Yotiao were associated with β2-AR in decreasing TGF-β1-induced collagen I upregulation, but not with PDE3 or PDE4.

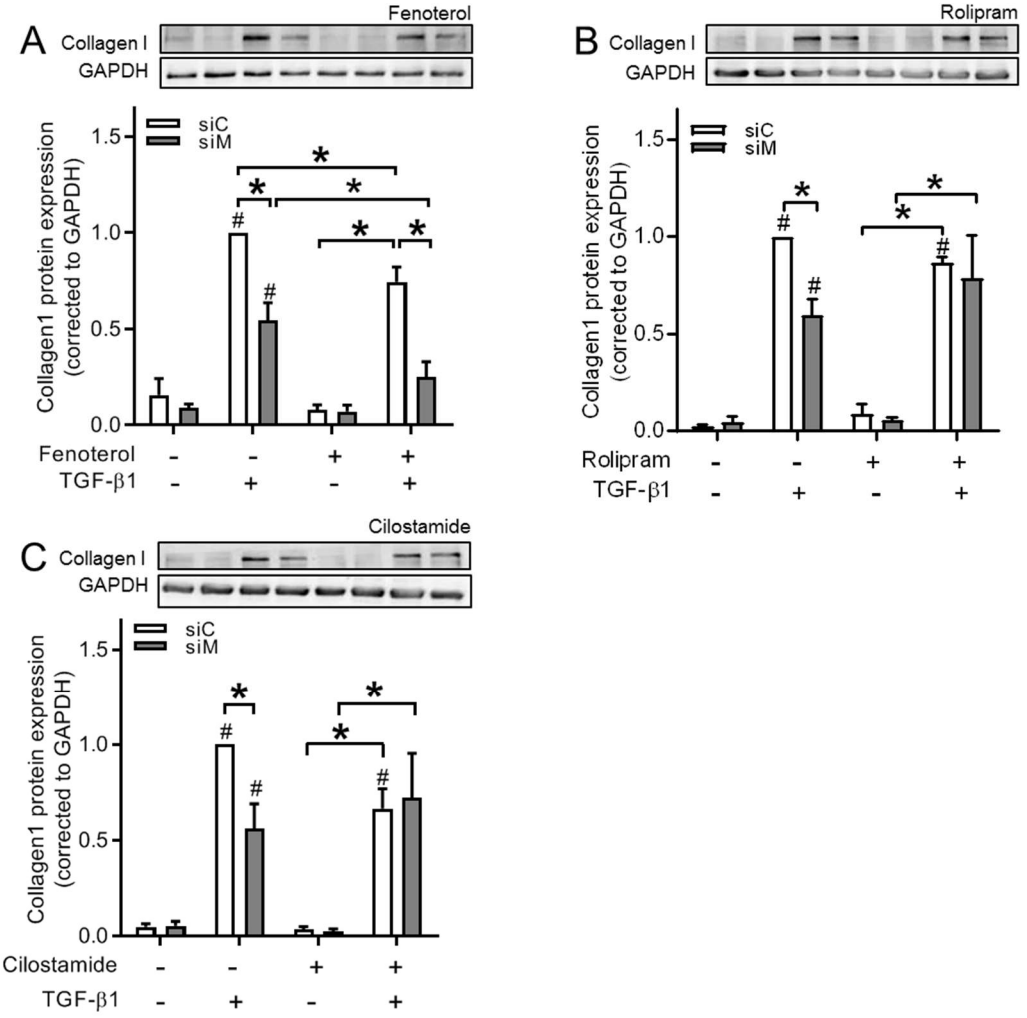

Figure 10. Combined Ezrin, AKAP95 and Yotiao silencing differentially blunted reduction of TGF-β1-induced collagen I elevation by fenoterol, rolipram and cilostamide in BEAS-2B cells. (A-C) Representative western blotting images and quantification of collagen I in cells pre-incubated with fenoterol (A) rolipram (B) or cilostamide (C) before TGF-β1 treatment. Data represent 4 independent experiments. Data are expressed as mean ± SEM, *: $p<0.05$; significantly different between indicated groups. #: $p<0.05$; significant difference compared to control groups.

Table 4. The comparison of Collagen I protein expression in co-silencing multiple AKAPs with or without cAMP donors.

Treatment	Collagen I		
	Control	siControl	siMultiple

	-TGF-β1	+TGF-β1	-TGF-β1	+TGF-β1	-TGF-β1	+TGF-β1
Control	0.18±0.04	1.00±0.00				
Fenoterol 10μM	0.23±0.07	0.71±0.06				
Rolipram 10μM	0.11±0.03	0.68±0.09				
Cilostamide 10μM	0.11±0.03	0.59±0.10				
			0.08±.03	1.00±0.00	0.04±0.01	0.25±0.06
Control			0.16±0.09	1.00±0.00	0.09±0.02	0.54±0.09
Fenoterol 10μM			0.08±0.02	0.75±0.08	0.07±0.03	0.25±0.08
Control			0.02±0.06	1.00±0.00	0.04±0.02	0.59±0.08
Rolipram 10μM			0.08±0.05	0.76±0.05	0.05±0.01	0.75±0.22
Control			0.04±0.01	1.00±0.00	0.05±0.02	0.55±0.13
Cilostamide 10μM			0.03±0.01	0.86±0.29	0.02±0.01	0.72±0.23

4. Discussion

In this study, we investigated the role of AKAPs in TGF-β1/CS-induced EMT in normal human bronchial epithelial BEAS-2B cells and primary HAE cells. We show that the physical interaction between AKAP and PKA is required for TGF-β1-induced EMT, a process characterized by reduced E-cadherin and increased collagen I expression. Relevant to the pathophysiology of COPD, CSE similarly induced EMT by stimulation the release of TGF-β1 and subsequnent activation of TGF-β1 signaling, which was needed to induce EMT. We found that gene and protein expression of Ezrin, AKAP95 and Yotiao were specifically altered by TGF-β1. Indeed, single knockdown of Ezrin, AKAP95 or Yotiao diminished TGF-β1-induced collagen I upregulation, which was further suppressed when they were simultaneously knocked down. Functionally, we report that co-silencing of Ezrin, AKAP95 and Yotiao inhibited TGF-β1-induced cell migration. In addition, co-silencing of Ezrin, AKAP95 and Yotiao further accelerated the effect of the β_2-AR but not of PDE3 or PDE4 on TGF-β1-induced collagen I upregulation.

Cigarette smoke, as one of the most important inducing factors in COPD, activates the EMT process, which contributes to COPD progression. Sohal et al. demonstrated that reticular basement membrane fragmentation, a key indicator of EMT *in vivo*, was significantly increased in current smokers with or without COPD as compared to never-smoking control subjects, which also positively correlated with smoking history [7]. Further investigation using immunohistochemistry indicated that fibroblast specific protein S100A4 was significantly increased in reticular basement membrane clefts in smokers, highlighting the active EMT process in the fragmented reticular basement membrane of smokers and COPD patients [7]. This finding was further confirmed by another *in vivo* study, in which significant upregulation of mesenchymal marker vimentin was observed within the small airway epithelium of smokers and COPD subjects [25]. In addition, Milara et al. showed that EMT was increased in primary

Peer-reviewed version available at Cells 2020, 9, 356; doi:10.3390/cells9020356

bronchial epithelial cells of the small bronchi of smokers and COPD patients as compared to the small bronchi of non-smoking control subjects, indicating that EMT was induced by CS exposure [6]. However, the mechanism of CS-induced EMT in airway epithelial cells is still poorly understood. We show that CS exposure increases TGF-β1 release, which is consistent with a previous study [6]. Also, we demonstrate that CS exposure enhanced phosphorylation of SMAD2 and SMAD3 (not shown), which are the key downstream effectors in TGF-β signaling. Also, CS extract-induced E-cadherin loss was inhibited by pre-treatment with a TGF-β neutralizing antibody. CS exposure also activated cell migration in BEAS-2B cells, which could be decreased when Ezrin, AKAP95 and Yotiao were co-silenced. This indicates that Ezrin, AKAP95 and Yotiao are involved in CS-promoted EMT.

It has been demonstrated that the membrane-cytoskeleton linker Ezrin plays a vital role in cell migration and invasion by modulating the assembly of cytoskeleton elements through Rho GTPase signaling to regulate cytoskeletal organization and cellular phenotypical alterations [26-28]. Recent studies have shown that regulation of Ezrin might be altered in pulmonary diseases. The protein expression of Ezrin was unaltered in the bronchoalveolar lavage fluid of COPD patients [29], while Ezrin protein expression was higher in the epithelium samples from COPD patients compared to the samples from healthy individuals [30]. Additionally, Ezrin protein was decreased in asthmatic exhaled breath condensate and serum compared to non-asthmatic control subjects [31]. Importantly, it was pointed out by several studies that the subcellular location of Ezrin, rather than its expression levels correlates with its function [32,33]. Such aspects were not studied in BEAS-2B cells yet. Ezrin overexpression was associated with enhanced tumor aggressiveness, while knockdown of Ezrin expression reduced proliferation, migration and invasion of cancer cells [34-36]. Suppression of Ezrin expression by siRNA prevented the morphological changes, actin filament remodeling and E-cadherin loss induced by TGF-β1 in alveolar epithelial A549 cells [17]. Surprisingly in our study, knockdown of Ezrin decreased TGF-β1-induced collagen I upregulation, while it did not prevent TGF-β1-induced E-cadherin decrease in BEAS-2B cells, which contrasts to the earlier-mentioned studies using A549 cells [17]. It is important to note that A549 cells are human alveolar basal epithelial cells, while BEAS-2B cells are normal human epithelial cells localizing in bronchus. The specific location in the tissue may partly explain the different observation regarding the function of Ezrin in TGF-β1-induced E-cadherin decrease between our study and those reported earlier.

AKAP95, also known as AKAP8, resides in the nucleus and is involved in DNA replication and controls expression of several proteins that regulate the cell cycle [15,37]. TGF-β1 has been found to increase cell proliferation in the lung structural cells [38,39]. In the current study, we observed that knockdown of AKAP95 decreased TGF-β1-induced collagen I production. It is tempting to speculate that this process might be linked to the fact that silencing of AKAP95 inhibited TGF-β1-induced cell proliferation in BEAS-2B cells.

Yotiao, also known as AKAP9, is involved in the development and metastasis of several cancers, including breast cancer [40], lung cancer [41], melanomas [42], thyroid carcinomas [43,44], and colorectal cancer [18]. Knockdown of Yotiao by short hairpin RNA inhibited tumor growth in mice, which was partly due to the fact that Yotiao knockdown induced an increase in the epithelial marker E-cadherin and decreased mesenchymal markers N-cadherin and vimentin, indicating that Yotiao plays a crucial role in EMT [18]. We found that siRNA-mediated knockdown of Yotiao significantly decreased TGF-β1-induced upregulation of the mesenchymal marker collagen I, indicating that

Yotiao acts as a potential target to prevent EMT. Surprisingly, TGF-β1-induced suppression of E-cadherin was further decreased when Yotiao was silenced, which seemed to be conflicting with previous observations [18]. However, earlier we showed that Yotiao and E-cadherin co-localize at the cell membrane of human bronchial epithelial 16HBE cells, highlighting the importance of Yotiao on epithelial barrier function [19]. Together with this finding, our observation in BEAS-2B cells emphasized the importance of Yotiao on cell membrane maintenance.

In the current study, distinct cAMP compartments were differentially activated by the β_2-agonist fenoterol, the PDE4 inhibitor rolipram, the PDE3 inhibitor cilostamide and dbcAMP. We found that TGF-β1-induced collagen I upregulation was suppressed when cAMP donors were applied. Moreover, co-silencing of Ezrin-AKAP95-Yotiao further decreased TGF-β1-induced collagen I upregulation, implicating that these AKAPs may act in concert with the β_2-AR in diminishing TGF-β1-induced collagen I induction. β_2-AR binds to the ezrin/radixin/moesin-binding phosphoprotein 50 (also referred to as NHERF) complex through their PDZ motifs in airway epithelial cells, highlighting the association between Ezrin and β_2-AR, which is in line with our findings [45]. Intriguingly, co-silencing of Ezrin-AKAP95-Yotiao silencing did not alter the effects of the PDE4 inhibitor rolipram and the PDE3 inhibitor cilostamide on collagen I protein expression, strongly suggesting that distinctly AKAP-defined compartments determine the functional outcome of the β_2-AR compared to PDE3 and PDE4 in the TGF-β1-induced EMT process (shown in **Fig. 11**). More investigations are needed to study the difference between β_2-AR, PDE3 and PDE4. In addition, chronic lung diseases such as COPD are discussed in the context of a spectrum of EMT states [46], which would be reflected in our current study by the selective role of Ezrin-AKAP95-Yotiao in diminishing TGF-β1-induced collagen I deposition, without restoration of E-cadherin.

5. Conclusion

Our study demonstrates that the AKAP family members Ezrin, AKAP95 and Yotiao play essential roles in TGF-β1-induced EMT. The co-silencing of Ezrin, AKAP95 and Yotiao inhibits TGF-β1-induced collagen I production in human bronchial epithelial BEAS-2B cells. Functionally, we show that Ezrin, AKAP95 and Yotiao are required for TGF-β1-induced cell migration. Importantly, Ezrin, AKAP95 and Yotiao seem to act in concert with the β_2-AR but not PDE3 or PDE4 in decreasing TGF-β1-induced collagen I upregulation. CS, as an important risk factor for COPD, induces TGF-β1 release, thereby activating the TGF-β1 signaling pathway, which contributes to EMT progression. Thus, Ezrin, AKAP95 and Yotiao, represent promising therapeutic targets to inhibit bronchial EMT in COPD, possibly in combination with already existing therapies such as β_2-agonists and PDE4 inhibitors.

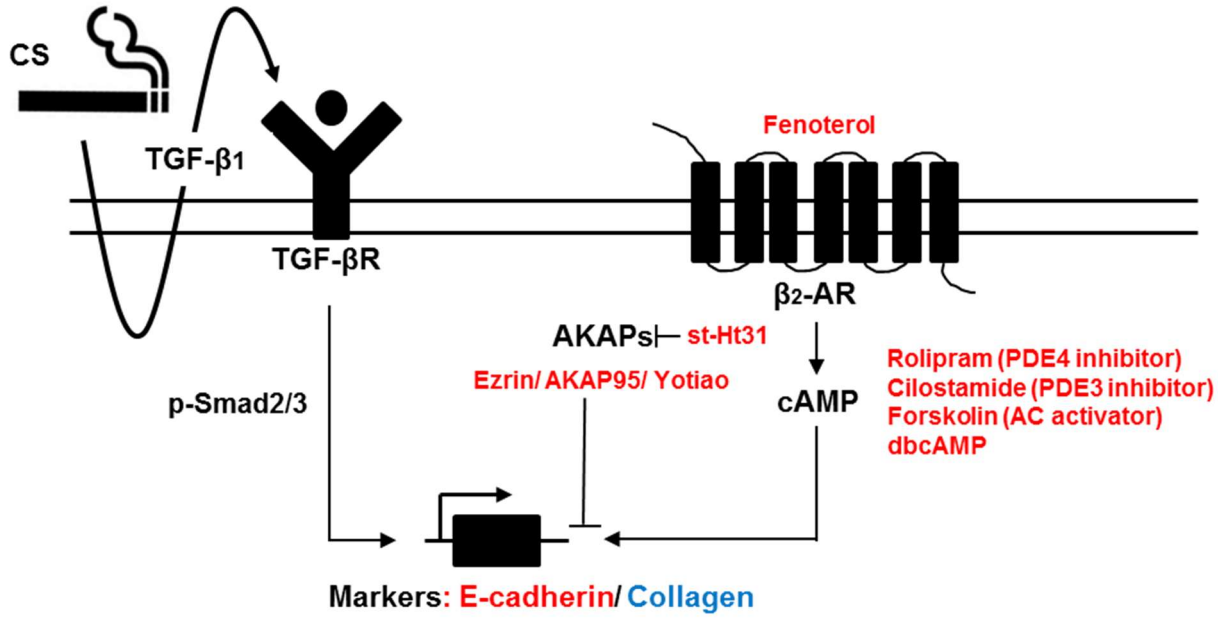

Figure 11. Proposed molecular mechanism explaining the role of different cAMP compartments in TGF-β1/CS-induced EMT in BEAS-2B cells. CS exposure induces TGF-β1 release, which in turn activates EMT via SMAD-dependent pathway. AKAPs, especially focusing on TGF-β1 sensitive AKAPs, Ezrin, AKAP95 and Yotiao, are involved in TGF-β1-induced collagen I upregulation. Elevation of cAMP by fenoterol, rolipram and cilostamide differentially diminish TGF-β1-induced *EMT*. Importantly, co-silencing of Ezrin, AKAP95 and Yotiao is associated with β_2-AR but not PDE3 or PDE4 in decreasing TGF-β1-induced collagen I upregulation.

Supplementary Materials: The following are available online at www.mdpi.com/xxx/s1, Figure S1: Silencing of Ezrin, AKAP95 and Yotiao (mRNA); A-C); protein (D,E). Figure S2: Role of Ezrin, AKAP95 and Yotiao in CS-induced cell migration (A) and proliferation B).

Author Contributions: H.Z. carried out the experiments, formal data analysis and supported writing the manuscript, including preparation of the figures. C.H.T.J.v.d.Veen performed experiments, supported data analysis. L.H. performed the TGF Elisa. K.N.F. supported the measurements with xCelligence. W.J.P. supported data collection. H.M. supported manuscript writing. V.O.N supported critical proof-reading of the manuscript. M.S. planned the research, analyzed the data and prepared the final manuscript version. All authors reviewed the manuscript and conceived manuscript polishing.

Funding: This work was supported by the Ubbo Emmius Programme (grant to H.Z), the Deutsche Forschungsgemeinschaft (grant to M.S) and the Gertraud und Heinz-Rose Stiftung (grant to V.O.N.).

Acknowledgments: We thank Ksenia A. Myacheva, Lennard Ringnalda, Celine Warries and Melissa van Es for their excellent experimental performance and Danial Afsharzadeh for support with xCELLigence. We also thank Alexander Martin Heberle and Miriam Langelaar-Makkinje for their kind help with Incucyte.

Conflicts of Interest: The authors declare no conflict of interest.

References

1. Vogelmeier, C.F.; Criner, G.J.; Martinez, F.J.; Anzueto, A.; Barnes, P.J.; Bourbeau, J.; Celli, B.R.; Chen, R.; Decramer, M.; Fabbri, L.M., et al. Global Strategy for the Diagnosis, Management, and Prevention of Chronic Obstructive Lung Disease 2017 Report. GOLD Executive Summary. *Am J Respir Crit Care Med* **2017**, *195*, 557-582. [CrossRef]
2. Kalluri, R.; Neilson, E.G. Epithelial-mesenchymal transition and its implications for fibrosis. *J Clin Invest* **2003**, *112*, 1776-1784. [CrossRef]
3. Kim, K.K.; Kugler, M.C.; Wolters, P.J.; Robillard, L.; Galvez, M.G.; Brumwell, A.N.; Sheppard, D.; Chapman, H.A. Alveolar epithelial cell mesenchymal transition develops in vivo during pulmonary fibrosis and is regulated by the extracellular matrix. *Proc Natl Acad Sci U S A* **2006**, *103*, 13180-13185. [CrossRef]
4. Zeisberg, M.; Neilson, E.G. Biomarkers for epithelial-mesenchymal transitions. *J Clin Invest* **2009**, *119*, 1429-1437. [CrossRef]
5. Zuo, H.; Cattani-Cavalieri, I.; Valenca, S.S.; Musheshe, N.; Schmidt, M. Function of cAMP scaffolds in obstructive lung disease: Focus on epithelial-to-mesenchymal transition and oxidative stress. *Br J Pharmacol* **2019**, *176*, 2402-2415. [CrossRef]
6. Milara, J.; Peiro, T.; Serrano, A.; Cortijo, J. Epithelial to mesenchymal transition is increased in patients with COPD and induced by cigarette smoke. *Thorax* **2013**, *68*, 410-420. [CrossRef]
7. Sohal, S.S.; Reid, D.; Soltani, A.; Ward, C.; Weston, S.; Muller, H.K.; Wood-Baker, R.; Walters, E.H. Reticular basement membrane fragmentation and potential epithelial mesenchymal transition is exaggerated in the airways of smokers with chronic obstructive pulmonary disease. *Respirology* **2010**, *15*, 930-938. [CrossRef]
8. Sohal, S.S.; Walters, E.H. Epithelial mesenchymal transition (EMT) in small airways of COPD patients. *Thorax* **2013**, *68*, 783-784. [CrossRef]
9. Kalluri, R.; Weinberg, R.A. The basics of epithelial-mesenchymal transition. *J Clin Invest* **2009**, *119*, 1420-1428. [CrossRef]
10. Bartis, D.; Mise, N.; Mahida, R.Y.; Eickelberg, O.; Thickett, D.R. Epithelial-mesenchymal transition in lung development and disease: does it exist and is it important? *Thorax* **2014**, *69*, 760-765. [CrossRef]
11. Jansen, S.R.; Poppinga, W.J.; de Jager, W.; Lezoualc'h, F.; Cheng, X.; Wieland, T.; Yarwood, S.J.; Gosens, R.; Schmidt, M. Epac1 links prostaglandin E2 to beta-catenin-dependent transcription during epithelial-to-mesenchymal transition. *Oncotarget* **2016**, *7*, 46354-46370. [CrossRef]
12. Jolly, M.K.; Ware, K.E.; Gilja, S.; Somarelli, J.A.; Levine, H. EMT and MET: necessary or permissive for metastasis? *Mol Oncol* **2017**, *11*, 755-769. [CrossRef]
13. Nieto, M.A. The ins and outs of the epithelial to mesenchymal transition in health and disease. *Annu Rev Cell Dev Biol* **2011**, *27*, 347-376. [CrossRef]
14. Beene, D.L.; Scott, J.D. A-kinase anchoring proteins take shape. *Curr Opin Cell Biol* **2007**, *19*, 192-198. [CrossRef]
15. Skroblin, P.; Grossmann, S.; Schafer, G.; Rosenthal, W.; Klussmann, E. Mechanisms of protein kinase A anchoring. *Int Rev Cell Mol Biol* **2010**, *283*, 235-330. [CrossRef]

16. Poppinga, W.J.; Munoz-Llancao, P.; Gonzalez-Billault, C.; Schmidt, M. A-kinase anchoring proteins: cAMP compartmentalization in neurodegenerative and obstructive pulmonary diseases. *Br J Pharmacol* **2014**, *171*, 5603-5623. [CrossRef]
17. Chen, M.J.; Gao, X.J.; Xu, L.N.; Liu, T.F.; Liu, X.H.; Liu, L.X. Ezrin is required for epithelial-mesenchymal transition induced by TGF-beta1 in A549 cells. *Int J Oncol* **2014**, *45*, 1515-1522. [CrossRef]
18. Hu, Z.Y.; Liu, Y.P.; Xie, L.Y.; Wang, X.Y.; Yang, F.; Chen, S.Y.; Li, Z.G. AKAP-9 promotes colorectal cancer development by regulating Cdc42 interacting protein 4. *Biochim Biophys Acta* **2016**, *1862*, 1172-1181. [CrossRef]
19. Oldenburger, A.; Poppinga, W.J.; Kos, F.; de Bruin, H.G.; Rijks, W.F.; Heijink, I.H.; Timens, W.; Meurs, H.; Maarsingh, H.; Schmidt, M. A-kinase anchoring proteins contribute to loss of E-cadherin and bronchial epithelial barrier by cigarette smoke. *Am J Physiol Cell Physiol* **2014**, *306*, C585-597. [CrossRef]
20. van Wetering, S.; van der Linden, A.C.; van Sterkenburg, M.A.; Rabe, K.F.; Schalkwijk, J.; Hiemstra, P.S. Regulation of secretory leukocyte proteinase inhibitor (SLPI) production by human bronchial epithelial cells: increase of cell-associated SLPI by neutrophil elastase. *J Investig Med* **2000**, *48*, 359-366.
21. Poppinga, W.J.; Heijink, I.H.; Holtzer, L.J.; Skroblin, P.; Klussmann, E.; Halayko, A.J.; Timens, W.; Maarsingh, H.; Schmidt, M. A-kinase-anchoring proteins coordinate inflammatory responses to cigarette smoke in airway smooth muscle. *Am J Physiol Lung Cell Mol Physiol* **2015**, *308*, L766-775. [CrossRef]
22. Keenan, C.R.; Langenbach, S.Y.; Jativa, F.; Harris, T.; Li, M.; Chen, Q.; Xia, Y.; Gao, B.; Schuliga, M.J.; Jaffar, J., et al. Casein Kinase 1delta/epsilon Inhibitor, PF670462 Attenuates the Fibrogenic Effects of Transforming Growth Factor-beta in Pulmonary Fibrosis. *Front Pharmacol* **2018**, *9*, 738. [CrossRef]
23. Ruijter, J.M.; Ramakers, C.; Hoogaars, W.M.; Karlen, Y.; Bakker, O.; van den Hoff, M.J.; Moorman, A.F. Amplification efficiency: linking baseline and bias in the analysis of quantitative PCR data. *Nucleic Acids Res* **2009**, *37*, e45. [CrossRef]
24. Mihailichenko, D., Pertseva, T. Influence of tobacco-smoking on serum level of transforming growth factor (TGF) beta 1 in COPD patients. *Eur. Respir. J. 50, PA3602* **2017**.
25. Wang, Q.; Wang, Y.; Zhang, Y.; Zhang, Y.; Xiao, W. The role of uPAR in epithelial-mesenchymal transition in small airway epithelium of patients with chronic obstructive pulmonary disease. *Respir Res* **2013**, *14*, 67. [CrossRef]
26. Fehon, R.G.; McClatchey, A.I.; Bretscher, A. Organizing the cell cortex: the role of ERM proteins. *Nat Rev Mol Cell Biol* **2010**, *11*, 276-287. [CrossRef]
27. Ivetic, A.; Ridley, A.J. Ezrin/radixin/moesin proteins and Rho GTPase signalling in leucocytes. *Immunology* **2004**, *112*, 165-176. [CrossRef]
28. Tsukita, S.; Yonemura, S. ERM (ezrin/radixin/moesin) family: from cytoskeleton to signal transduction. *Curr Opin Cell Biol* **1997**, *9*, 70-75. [CrossRef]
29. Pastor, M.D.; Nogal, A.; Molina-Pinelo, S.; Melendez, R.; Salinas, A.; Gonzalez De la Pena, M.; Martin-Juan, J.; Corral, J.; Garcia-Carbonero, R.; Carnero, A., et al. Identification of proteomic signatures associated with lung cancer and COPD. *J Proteomics* **2013**, *89*, 227-237. [CrossRef]

30. Li, Q.; Li, N.; Liu, C.Y.; Xu, R.; Kolosov, V.P.; Perelman, J.M.; Zhou, X.D. Ezrin/Exocyst complex regulates mucin 5AC secretion induced by neutrophil elastase in human airway epithelial cells. *Cell Physiol Biochem* **2015**, *35*, 326-338. [CrossRef]
31. Jia, M.; Yan, X.; Jiang, X.; Wu, Y.; Xu, J.; Meng, Y.; Yang, Y.; Shan, X.; Zhang, X.; Mao, S., et al. Ezrin, a Membrane Cytoskeleton Cross-Linker Protein, as a Marker of Epithelial Damage in Asthma. *Am J Respir Crit Care Med* **2019**, *199*, 496-507. [CrossRef]
32. Perez, P.; Aguilera, S.; Olea, N.; Alliende, C.; Molina, C.; Brito, M.; Barrera, M.J.; Leyton, C.; Rowzee, A.; Gonzalez, M.J. Aberrant localization of ezrin correlates with salivary acini disorganization in Sjogren's Syndrome. *Rheumatology (Oxford)* **2010**, *49*, 915-923. [CrossRef]
33. Sarrio, D.; Rodriguez-Pinilla, S.M.; Dotor, A.; Calero, F.; Hardisson, D.; Palacios, J. Abnormal ezrin localization is associated with clinicopathological features in invasive breast carcinomas. *Breast Cancer Res Treat* **2006**, *98*, 71-79. [CrossRef]
34. Huang, H.Y.; Li, C.F.; Fang, F.M.; Tsai, J.W.; Li, S.H.; Lee, Y.T.; Wei, H.M. Prognostic implication of ezrin overexpression in myxofibrosarcomas. *Ann Surg Oncol* **2010**, *17*, 3212-3219. [CrossRef]
35. Li, Q.; Gao, H.; Xu, H.; Wang, X.; Pan, Y.; Hao, F.; Qiu, X.; Stoecker, M.; Wang, E.; Wang, E. Expression of ezrin correlates with malignant phenotype of lung cancer, and in vitro knockdown of ezrin reverses the aggressive biological behavior of lung cancer cells. *Tumour Biol* **2012**, *33*, 1493-1504. [CrossRef]
36. Saito, S.; Yamamoto, H.; Mukaisho, K.; Sato, S.; Higo, T.; Hattori, T.; Yamamoto, G.; Sugihara, H. Mechanisms underlying cancer progression caused by ezrin overexpression in tongue squamous cell carcinoma. *PLoS One* **2013**, *8*, e54881. [CrossRef]
37. Han, B.; Poppinga, W.J.; Schmidt, M. Scaffolding during the cell cycle by A-kinase anchoring proteins. *Pflugers Arch* **2015**, *467*, 2401-2411. [CrossRef]
38. Chen, G.; Khalil, N. TGF-beta1 increases proliferation of airway smooth muscle cells by phosphorylation of map kinases. *Respir Res* **2006**, *7*, 2. [CrossRef]
39. Yue, X.; Shan, B.; Lasky, J.A. TGF-beta: Titan of Lung Fibrogenesis. *Curr Enzym Inhib* **2010**, *6*. [CrossRef]
40. Frank, B.; Wiestler, M.; Kropp, S.; Hemminki, K.; Spurdle, A.B.; Sutter, C.; Wappenschmidt, B.; Chen, X.; Beesley, J.; Hopper, J.L., et al. Association of a common AKAP9 variant with breast cancer risk: a collaborative analysis. *J Natl Cancer Inst* **2008**, *100*, 437-442. [CrossRef]
41. Truong, T.; Sauter, W.; McKay, J.D.; Hosgood, H.D., 3rd; Gallagher, C.; Amos, C.I.; Spitz, M.; Muscat, J.; Lazarus, P.; Illig, T., et al. International Lung Cancer Consortium: coordinated association study of 10 potential lung cancer susceptibility variants. *Carcinogenesis* **2010**, *31*, 625-633. [CrossRef]
42. Kabbarah, O.; Nogueira, C.; Feng, B.; Nazarian, R.M.; Bosenberg, M.; Wu, M.; Scott, K.L.; Kwong, L.N.; Xiao, Y.; Cordon-Cardo, C., et al. Integrative genome comparison of primary and metastatic melanomas. *PLoS One* **2010**, *5*, e10770. [CrossRef]
43. Caria, P.; Vanni, R. Cytogenetic and molecular events in adenoma and well-differentiated thyroid follicular-cell neoplasia. *Cancer Genet Cytogenet* **2010**, *203*, 21-29. [CrossRef]
44. Lee, J.H.; Lee, E.S.; Kim, Y.S.; Won, N.H.; Chae, Y.S. BRAF mutation and AKAP9 expression in sporadic papillary thyroid carcinomas. *Pathology* **2006**, *38*, 201-204. [CrossRef]

45. Naren, A.P.; Cobb, B.; Li, C.; Roy, K.; Nelson, D.; Heda, G.D.; Liao, J.; Kirk, K.L.; Sorscher, E.J.; Hanrahan, J., et al. A macromolecular complex of beta 2 adrenergic receptor, CFTR, and ezrin/radixin/moesin-binding phosphoprotein 50 is regulated by PKA. *Proc Natl Acad Sci U S A* **2003**, *100*, 342-346. [CrossRef]

46. Jolly, M.K.; Ward, C.; Eapen, M.S.; Myers, S.; Hallgren, O.; Levine, H.; Sohal, S.S. Epithelial-mesenchymal transition, a spectrum of states: Role in lung development, homeostasis, and disease. *Dev Dyn* **2018**, *247*, 346-358. [CrossRef]